

Development of a New Condensation Heat Transfer Model for the Nearly Horizontal Tube of the APR+ PAFS (Passive Auxiliary Feed-water System)

Tae-hwan Ahn^a, Jae-Jun Jeong^a, Kyong-ho Kang^b, Yu-sun Park^b, Jong Cheon^c, Byong-Jo Yun^{a*}

^aSchool of mechanical Engineering, Pusan National University, Busan, 607-735, Korea,

^bKorea Atomic Energy Research Institute, 1045 Daedeok-daero, Yuseong-gu, Daejeon, 305-353, Korea

^cKHNP Central Research Institute, 1312-70-gil Yuseong-daero Yuseong-gu, Daejeon, 305-343, Korea

*Corresponding author: bjjun@pusan.ac.kr

1. Introduction

Recent nuclear power plants have adopted passive safety equipment driven by operating without any external power supply in case of accidents. It has high reliability because it works by natural forces such as gravity and other inherent energies of nature. The Korean 3.5 generation nuclear power plant named APR+ is planned to adopt the passive auxiliary feed-water system (PAFS), which is the safety equipment driven by natural circulation to remove the core decay heat to atmosphere through the condensing heat exchanger composed of the nearly horizontal tubes. Korea Atomic Energy Research Institute (KAERI) has recently conducted PASCAL experiment to confirm the performance of PAFS. From the work, it is founded that the condensation heat transfer coefficient predicted by best estimated safety analysis code MARS (Multi-dimensional Analysis of Reactor Safety) was underestimated compared to the experimental data [1]. Shah [2] correlation embedded in MARS code is the typical model using the empirical two-phase multiplier to determine condensation heat transfer coefficient for annular flow in the condensing tube. On the other hand, the PASCAL experiment indicated that a stratified-wavy flow generally tends to occur in the downward inclined tube of the condensation heat exchanger. Therefore, in order to improve the prediction capability of safety analysis codes for PAFS, the present study has proposed a new condensation heat transfer model package for the nearly horizontal tube, which determines mechanistically the local heat transfer coefficient based on the flow regimes.

2. Model Package

To estimate accurately the condensation heat transfer rate in the nearly horizontal tube, a new condensation heat transfer model package consisting of a one-dimensional separated flow model for a void fraction, a flow regime identification model, and the condensation heat transfer correlations has been developed in this study. The model package takes into consideration the inclination angle of the condensing tube and various flow regimes that are expected in the nearly horizontal tube.

2.1 Void Fraction Prediction

Void fraction was calculated by one-dimensional separated flow model (SFM). Assuming fully developed flow with one-dimensional steady state, the momentum equations of vapor and liquid phases are as follows.

$$-A_g \left(\frac{dP}{dz} \right) - \tau_{wg} S_g - \tau_i S_i + \rho_g A_g g \sin \theta = 0 \quad (1)$$

$$-A_l \left(\frac{dP}{dz} \right) - \tau_{wl} S_l + \tau_i S_i + \rho_l A_l g \sin \theta = 0 \quad (2)$$

Assuming the same pressure drop for the two phases, equations above can be expressed as follows.

$$\tau_{wg} \frac{S_g}{A_g} - \tau_{wl} \frac{S_l}{A_l} + \tau_i S_i \left(\frac{1}{A_l} + \frac{1}{A_g} \right) + (\rho_l - \rho_g) g \sin \theta = 0 \quad (3)$$

Here, A_x is the cross-sectional area and S_x is the wetted perimeter over which the shear stress acts. The symbols τ_w and τ_i are the wall shear stresses and interfacial shear stress respectively, and the subscripts g and l mean the gas and liquid phases.

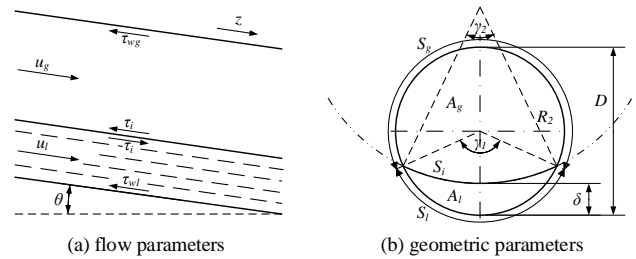


Fig. 1. Schematic descriptions of the stratified flow configuration and coordinate.

To determine the void fraction by the SFM, some closure relations are required for shear stresses and geometric parameters such as cross section areas and contact perimeters of each phase.

The phasic wall shear stresses are calculated by following single phase expressions.

$$\tau_{wg} = \frac{1}{2} f_g \rho_g u_g^2 \quad ; \quad \tau_{wl} = \frac{1}{2} f_l \rho_l u_l^2 \quad (4)$$

where the actual velocities of vapor and liquid are defined as a function of mass flux G , flow quality x , and void fraction α as shown below.

$$u_g = \frac{Gx}{\rho_g \alpha} \quad ; \quad u_l = \frac{G(1-x)}{\rho_l (1-\alpha)} \quad (5)$$

The friction factors f_g and f_l are obtained from the following Blasius' friction factor for a single phase.

$$f_g = \frac{c_g}{\text{Re}_g^{n_g}} \quad ; \quad f_l = \frac{c_l}{\text{Re}_l^{n_l}} \quad (6)$$

The Reynolds numbers were calculated based on the actual velocity and hydraulic equivalent diameter for each phase as follows.

$$\text{Re}_g = \frac{\rho_g u_g D_{hg}}{\mu_g} \quad ; \quad \text{Re}_l = \frac{\rho_l u_l D_{hl}}{\mu_l} \quad (7)$$

The hydraulic equivalent diameters in the Reynolds numbers were defined as follows.

$$D_{hg} = \frac{4A_g}{S_g + S_l} \quad ; \quad D_{hl} = \frac{4A_l}{S_l} \quad (8)$$

The constants and exponents in friction factors were defined as $c=16$, $n=1.0$ for the laminar flow; $c=0.046$, $n=0.2$ for the turbulent flow.

The interfacial shear stress was calculated from the following equation.

$$\tau_i = \frac{1}{2} f_g \rho_g |u_g - u_l| (u_g - u_l) \quad (9)$$

where the friction factor and density for the gas phase were used with the assumption by Taitel and Dukler [3].

The geometric parameters for the interface shape such as flow cross-section areas and wetted perimeters were defined for solving Eq. (3). Taitel and Dukler calculated these variables by assuming the flat interface shape. This assumption is valid when the shear stress effect on the interface is insignificant in the low flow condition. However, if the relative velocity between phases increases in the flow channel, the interface becomes far away from flat shape due to interfacial shear stress. In this study, to consider the interface change with respect to the flow as shown in Fig. 1 (b), the interface was considered as the ideal arc shape as mentioned above, and its geometrical characteristics was defined using the following relations.

$$\gamma_2 = -4 \tan^{-1} \left(\frac{\frac{D}{2} \cos \frac{\gamma_1}{2} - \frac{D}{2} + \delta}{\frac{D}{2} \sin \frac{\gamma_1}{2}} \right) \quad (10)$$

$$R_2 = \frac{\left(\frac{D}{2} \sin \frac{\gamma_1}{2} \right)}{\sin \frac{\gamma_2}{2}} \quad (11)$$

where the wetted angle γ_1 is calculated using the following correlation proposed by Hart et al. [4].

$$\gamma_1 = 2\pi \left(0.52(1-\alpha)^{0.374} + 0.26Fr^{0.58} \right) \quad (12)$$

where Froude number in equation above is

$$Fr = \frac{\rho_l u_l^2}{(\rho_l - \rho_g) g D \cos \theta} \quad (13)$$

By using Eqs. (10) ~ (13), the flow cross sections and perimeters of each phase can be calculated as follows.

$$A_g = \left(\pi D^2 / 4 \right) - \left(D^2 / 8 \right) (\gamma_1 - \sin \gamma_1) + \left(R_2^2 / 2 \right) (\gamma_2 - \sin \gamma_2) \quad (14)$$

$$A_l = \left(D^2 / 8 \right) (\gamma_1 - \sin \gamma_1) - \left(R_2^2 / 2 \right) (\gamma_2 - \sin \gamma_2) \quad (15)$$

$$S_g = \pi D - \gamma_1 (D/2) \quad (16)$$

$$S_l = \gamma_1 (D/2) \quad (17)$$

$$S_i = \gamma_2 R_2 \quad (18)$$

2.2 Flow Regimes

The expected flow regimes inside a horizontal tube during condensation are typically classified into annular flow, stratified-wavy flow, stratified-smooth flow, and intermittent regimes. In the PASCAL experiment, the annular flow was observed at the entrance region of the tube in which high convective steam flows, and then the stratified flow takes place sequentially by the accumulated condensate on the bottom of the tube because of gravity effect. There also exist complicated intermittent flow regimes such as slug, plug and bubbly flow depending on flow conditions in the typical horizontal tube. However, separated flow such as stratified-wavy flow tends to occur under moderate mass flux condition with downward inclination [1]. Therefore, in the present work, the flow regime was classified into three flow regimes, including annular flow, stratified-wavy flow, and stratified-smooth flow as shown in Fig. 2. For this, non-stratified flow regimes including the intermittent flow were treated as annular flow regime. The wetted angle represented by Hart et al. [4] is used to describe the concave interface in the range of 0 to more than 2π . Therefore, the flow regime was defined as the annular flow for the wetted angle over 2π which is the upper limit of geometric condition as shown in Fig. 2 (a). For the stratified-smooth flow regime, the following equation for wetted angle γ_s was defined from Eq. (10) by assuming $\gamma_2=0$ as the simple flat interface as shown in Fig. 2 (c).

$$\gamma_s = 2 \cos^{-1} (1 - 2\delta / D) \quad (19)$$

The wetted angle obtained from Eq. (18) is criterion for the transition from stratified-wavy flow to stratified-smooth flow. By adopting these, the void fraction and heat transfer coefficient have no discontinuity at the flow regime transition boundaries. Consequently, the following criteria were proposed for the flow regime transitions.

From annular flow to stratified-wavy flow:

$$1 = 0.52(1-\alpha)^{0.374} + 0.26Fr^{0.58} \quad (20)$$

From stratified-wavy flow to stratified-smooth flow:

$$\frac{\gamma_s}{2\pi} = 0.52(1-\alpha)^{0.374} + 0.26Fr^{0.58} \quad (21)$$

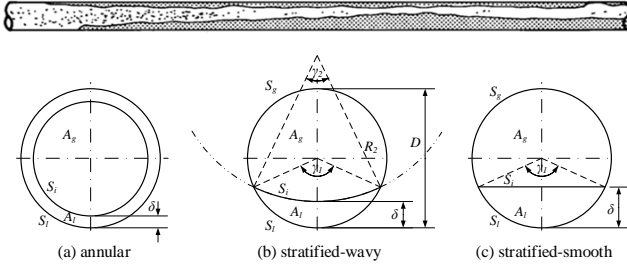


Fig. 2. Flow regimes during condensation in the horizontal tube.

2.3 Heat Transfer Coefficients

In the present study, heat transfer mechanisms inside the horizontal condensing tube are classified into film condensation and convective heat transfer. The film condensation occurs at the upper wall of the tube. On the other hand, the convective heat transfer occurs at both the lower part of the tube in the stratified flow and the entire wall in the annular flow. In this flow condition, the overall heat transfer coefficient is defined by averaging both film condensation and convective heat transfer coefficients with wetted angle γ_l as the weighting factor.

$$h = \frac{h_f(2\pi - \gamma_l) + h_c\gamma_l}{2\pi} \quad (22)$$

where

$$\begin{aligned} \gamma_l &= 2\pi && \text{for annular flow;} \\ \gamma_l &= 2\pi \left(0.52(1 - \alpha)^{0.374} + 0.26Fr^{0.58} \right) && \text{for stratified-wavy flow;} \\ \gamma_l &= \gamma_s && \text{for stratified-smooth flow} \end{aligned}$$

2.3.1 Film Condensation Heat Transfer Coefficient

Film condensation heat transfer correlation was based on the following average Nusselt [5] integral analysis, which formulates liquid film flowing down along the vertical plate.

$$\overline{Nu} = \frac{\overline{h}L}{k_l} = 0.943 \left[\frac{g\rho_l(\rho_l - \rho_g)h_{fg}L^3}{k_l\mu_l(T_{sat} - T_w)} \right]^{0.25} \quad (23)$$

Later, Dhir and Lienhard [6] proposed a new model coefficient 0.729 for the condensate film at the outside wall of a horizontal cylinder instead of conventional value coefficient 0.943 in the Eq. (22). However, the Nusselt-type correlation could not take into account the interfacial shear effects arisen by high convective vapor flow, because it was developed under the laminar flow conditions. To overcome this drawback, a new film condensation correlation which could take into consideration the interfacial shear stress effect was proposed by adding the vapor phase Reynolds number to the Nusselt-type correlation as follows.

$$h_f = 0.729 \left(1 + 8.9 \times 10^{-4} Re_g^{0.57} \right) \left(\frac{g\rho_l(\rho_l - \rho_g)h_{fg}k_l^3}{\mu_l D(T_{sat} - T_w)} \right)^{0.25} \quad (24)$$

Fig. 3 shows the tendency of the condensation heat transfer coefficients according to the vapor Reynolds number. The model coefficients of the additional terms for the consideration of the shear stress effect of a vapor flow was determined by means of the regression analysis against available data obtained from PASCAL [1] and ATLAS PAFS [7], [8] experiments. The proposed film condensation correlation maintains consistency with the Nusselt-type correlation suggested by Dhir and Lienhard [6], in the absence of vapor flow.

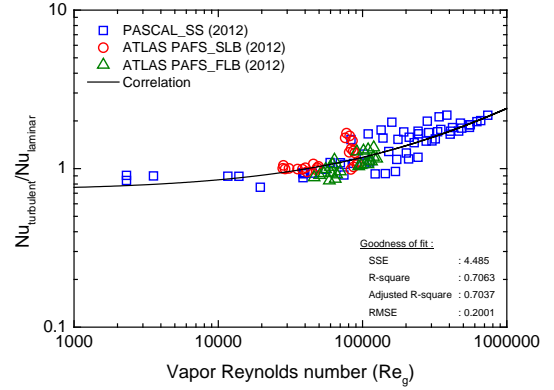


Fig. 3. Correlation of Nusselt numbers ratio as a function of vapor Reynolds number.

2.3.2 Convective Heat Transfer Coefficient

Dittus and Boelter [9] correlation for turbulent single-phase heat transfer was applied to convective heat transfer of condensate flowing along the bottom of the tube. The actual Reynolds number and hydraulic diameter of liquid phase were used in the correlation as follows.

$$h_c = 0.023 Re_l^{0.8} Pr_l^{0.3} \left(\frac{k_l}{D_{hl}} \right) \quad (25)$$

3. Evaluation of Model Package

The newly developed condensation model package was evaluated against available experimental database. Both of the void fraction and flow regime identification models were evaluated using the published data for the adiabatic air-water flow conditions. And then the condensation heat transfer model package was comprehensively assessed by comparing condensation data obtained under the steam-water condition. The prediction capability is quantified by following average and mean deviations.

$$\varepsilon_{ave} = \frac{1}{n} \sum_1^n \left[\frac{(h_{pre} - h_{exp})}{h_{exp}} \right] \times 100 \quad (26)$$

$$\varepsilon_{mean} = \frac{1}{n} \sum_1^n \left[\frac{|h_{pre} - h_{exp}|}{h_{exp}} \right] \times 100 \quad (27)$$

The average deviation, defined by Eq. (25), served as a common index to indicate the bias level of the predicted deviation. On the contrary, the mean deviation,

defined by Eq. (26), was used as an index to indicate the average size of error, which occurred due to the usage of absolute values.

3.1 Void Fraction Evaluation

The void fraction data used in the evaluation are listed in Table 1. Most of data were obtained in the nearly horizontal tube with downward inclination angle ranging from 0 to 3°. In the downward tube, the void fraction tends to be higher even in the extreme condition as flow quality $x=0$ due to the effect of gravity. It is worth noting that present void fraction model based on SFM takes into account the effect of gravity in the nearly horizontal tube. The comparison result is shown in Fig. 4 and percent deviations are also tabulated in the Table 1. It shows that present model predicts the local

void fraction within 5% of mean deviation against experimental data.

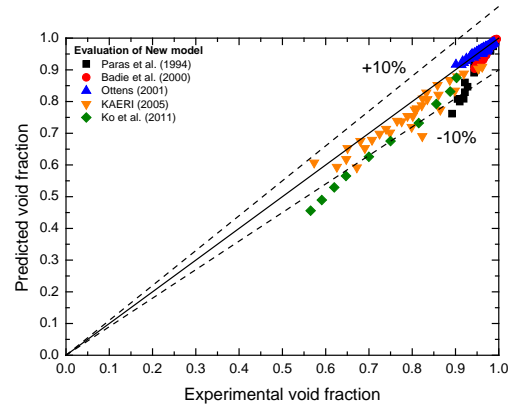


Fig. 4. Comparison of the void fraction predictions with experimental data.

TABLE I: Summary of data analyzed for void fraction

Data of	Fluid	Inclination	I.D. (mm)	Flow quality	No. of data points	ϵ_{avg} (%)	ϵ_{mean} (%)
Paras et al. [10]	Air-Water	Horizontal	50.8	0.1~0.6	19	-5	5
Badie et al. [11]	Air-Water(Oil)	Horizontal	78	0~0.3	66	-2.3	2.4
Ottens et al. [12]	Air-Water(Glycerol)	1° downward ~ horizontal	52	0.3~0.8	59	0.2	0.5
Yun et al. [13]	Air-Water	Horizontal	80	0~0.3	32	-3.5	4.2
Ko et al. [14]	Air-Water	3° downward ~ horizontal	45	0	10	-10.9	10.9
Total number of data points					186		
Overall average value of all date sets						-4.3	4.6

TABLE II: Summary of data analyzed for heat transfer coefficient

Data of	Fluid	ID (mm)	Inclination	Mass flux (kg/m ² s)	Reduced pressure	No. of data	Percent deviation (%)					
							Top h		Bottom h		Overall h	
							ϵ_{avg}	ϵ_{mean}	ϵ_{avg}	ϵ_{mean}	ϵ_{avg}	ϵ_{mean}
PASCAL_SS [1]	Water	44.8	3° downward	72~329	0.04~0.30	66	3.2	12.9	-19	31.3	-16	20.1
ATLAS PAFS_SLB [7]	Water	30.8	3° downward	69~88	0.10~0.17	24	-5.3	10.1	-2.2	11.2	-4.2	8.8
ATLAS PAFS_FLB [8]	Water	30.8	3° downward	79~118	0.13~0.29	24	8.5	11.7	-1.5	11.1	3.3	8
Wu* [16]	Water	27.5	Horizontal	10~80	0.02	49	76.3	76.9	-12.4	21.9	59.2	59.2
JAEA PCCS* [17]	Water	29	Horizontal	73	0.03	14					49.2	55.9
Total number of data points						177						
Overall average value of all date sets							20.7	27.9	-8.8	18.9	18.3	30.4

*1% of non-condensable gas is contained in the steam flow

3.2 Flow Regime Evaluation

The flow regime identification model was evaluated using Shoham [15] experimental data. In the test, flow regime data were obtained according to the various channel inclination angles under the atmospheric air-water flow condition. The inner diameter of test channel was 51 mm. Fig. 5 shows the evaluation results in the horizontal and 1° downward inclination conditions, respectively. As shown in the figures, present flow regime model shows reasonable prediction capability to the change of channel inclination angle. However, there are still differences with the experimental data. It is mainly caused by uncertainty of the wetted angle model and it should be improved for the better prediction.

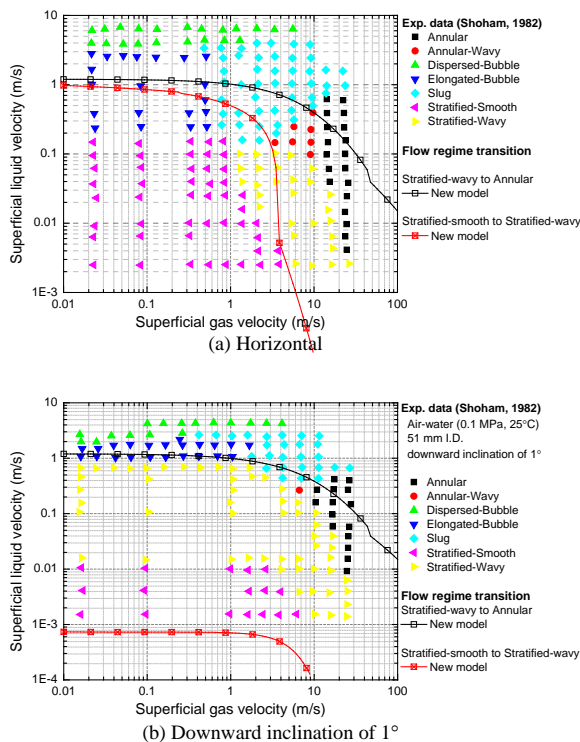


Fig. 5. Comparison of flow regime transitions with data available.

3.3 Heat Transfer Coefficient Evaluation

The experimental data used in the evaluation of condensation heat transfer correlations for the nearly horizontal tube are summarized in Table 2. All data in the Table are obtained from steam condensation tests in the nearly horizontal tube of which downward inclination angle is ranging from 0 to 3°. Among them, PASCAL [1] and ATLAS PAFS [7], [8] tests were conducted by KAERI in the prototypical flow conditions to validate the performance of PAFS for the APR+. In addition to, Wu [16] and the JAEA PCCS [17] were assessed for the verification of present model in the relatively lower pressure conditions. Fig. 6 (a) shows the comparison of heat transfer coefficients at the top and bottom of the condensation tube with

experimental data. Additionally, the overall heat transfer coefficient was also compared in the Fig. 6 (b). As tabulated in Table. 2, the percent deviation between model and data is less than 31% in terms of overall heat transfer coefficients.

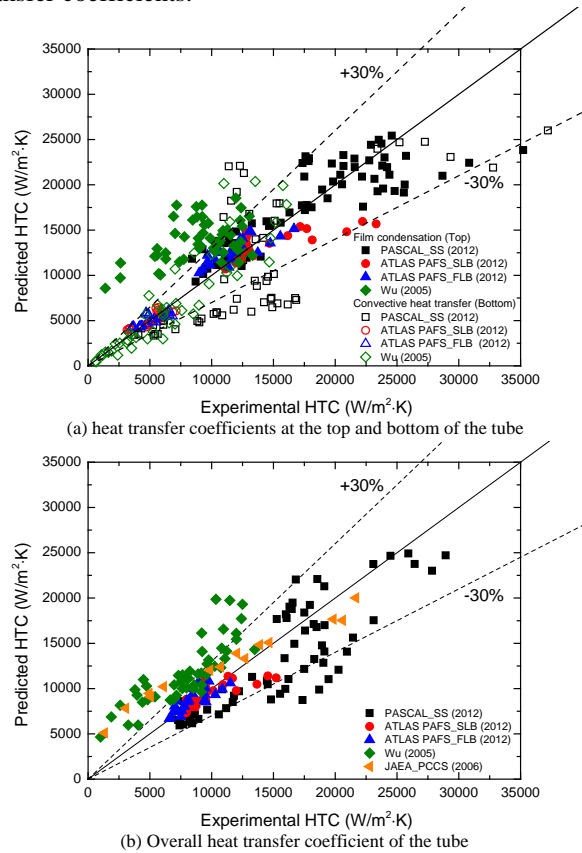


Fig. 6. Comparison of heat transfer coefficient predictions with data available.

4. Conclusions

To enhance prediction capability of one-dimensional best estimated code MARS for the PAFS of the Korean 3.5 generation nuclear power plant APR+, a new condensation heat transfer model package has been developed. The model package consists of the one-dimensional separated model for the void fraction, a flow regime model based on wetted angle, and the condensation heat transfer correlations. The model package considers the inclination angle of the condensing tube and various flow regimes that are expected in the tube during condensation process. Especially, the new model package treats independently film condensation and convective heat transfer phenomena in the upper and lower parts of the horizontal condensing tube respectively. For this, a film condensation model taking account interfacial shear stress effect was proposed based on the Nusselt's film condensation model.

The model package was compared against experimental data. The results indicated that present model package predicts available experimental data within a mean deviation of approximately 31%

ACKNOWLEDGMENTS

This work was supported by Nuclear Research & Development Program of the NRF (National Research Foundation of Korea) grant funded by the MSIP (Ministry of Science, ICT and Future Planning) and by the Nuclear Safety Research Center Program of the KORSAFe grant funded by Nuclear Safety and Security Commission (NSSC) of the Korean government (Grant code: NRF-2012M2A8A4055548, 1305011).

NOMENCLATURE

A	cross-sectional area (m^2)
c	constant in the friction factor
c_p	specific heat at constant pressure (J/kg-K)
D	tube inner diameter (m)
Fr	Froude number
f	friction factor
G	total mass flux of vapor and liquid (kg/m^2 -s)
g	gravity acceleration (m/s^2)
h	heat transfer coefficient (W/m^2 -K)
h_{fg}	enthalpy of vaporization (J/kg)
k	thermal conductivity (W/m -K)
n	exponent in the friction factor
Nu	Nusselt number (hD/k)
P	pressure (N/m^2)
Pr	Prandtl number, μ_p/k
R	radius (m)
Re	Reynolds number, $\rho u D/\mu$
S	wetted perimeter (m)
T	temperature (K)
u	actual velocity (m/s)
x	vapor flow quality
z	coordinate in the downstream direction

Greek Symbols

α	void fraction of vapor
γ	wetted angle (rad)
δ	liquid film thickness
θ	the inclination angle, positive for downward flow
μ	dynamic viscosity (N -s/ m^2)
ρ	density (kg/m^3)
τ	shear stress (N/m^2)

Subscripts and Superscripts

c	convective heat transfer
f	film condensation
g	gas phase
h	hydraulic equivalent
i	interface
l	liquid phase
s	stratified-smooth flow
sat	saturation
w	wall
1	the circle of tube
2	the eccentric circle

REFERENCES

- [1] S. Kim, B. U. Bae, Y. J. Cho, Y. S. Park, K. H. Kang and B. J. Yun, An experimental study on the validation of cooling capability for the Passive Auxiliary Feedwater System (PAFS) condensation heat exchanger, Nuclear Engineering and Design, Vol. 260, p. 54, 2013.
- [2] M. M. Shah, A general correlation for heat transfer during film condensation inside pipes, International Journal of Heat and Mass Transfer, Vol. 22.4, p. 547, 1979.
- [3] Y. Taitel, and A. E. Dukler, A model for predicting flow regime transitions in horizontal and near horizontal gas-liquid flow, AIChE Journal, Vol. 22.1, p. 47, 1976.
- [4] J. P. Hart, P. J. Hamersma, and J. M. H. Fortuin, Correlations predicting frictional pressure drop and liquid holdup during horizontal gas-liquid pipe flow with a small liquid holdup, International journal of multiphase flow, Vol. 15.6, p. 947, 1989.
- [5] W. Nusselt, Surface condensation of water vapour, Zeitschrift Des Vereines Deutscher Ingenieure, Vol. 60, p. 541, 1916.
- [6] V. Dhir and J. Lienhard, Laminar film condensation on plane and axisymmetric bodies in nonuniform gravity, Journal of Heat Transfer, Vol. 93, p. 97, 1971.
- [7] S. Kim, et al., Integral effect test on operational performance of the PAFS (Passive Auxiliary Feed-water System) for a SLB (Steam Line Break) accident, KAERI/TR-4768, (2012).
- [8] B. U. Bae, et al., Integral effect test on operational performance of the PAFS (Passive Auxiliary Feed-water System) for a FLB (Feed-water Line Break) accident, KAERI/TR-4757, (2012).
- [9] F. W. Dittus and L. M. K. Boelter, Heat transfer in automobile radiator of the tube type, Publication in Engineering, University of California, Berkley, Vol. 2, p. 250, 1930.
- [10] S. V. Paras, N. A. Vlachos, and A. J. Karabelas, Liquid layer characteristics in stratified—Atomization flow, International journal of multiphase flow, Vol. 20.5, p. 939, 1994.
- [11] S. Badie, C. P. Hale, C. J. Lawrence, and G. F. Hewitt, Pressure gradient and holdup in horizontal two-phase gas-liquid flows with low liquid loading, International journal of multiphase flow, Vol. 26.9, p. 1525, 2000.
- [12] M. Ottens, H. C. J. Hoefsloot, and P. J. Hamersma, Correlations predicting liquid hold-up and pressure gradient in steady-state (nearly) horizontal co-current gas-liquid pipe flow, Chemical Engineering Research and Design, Vol. 79.5, p. 581, 2001.
- [13] B. J. Yun, D. J. Euh, K. H. Kang, C. H. Song and W. P. Baek, Measurement of the single and two phase flow using a newly developed average bidirectional flow tube. Nuclear Engineering and Technology Vol. 37.6, p. 595, 2005.
- [14] M. S. Ko, et al., Preparatory Research on Flow Regime Transition in an Inclined Pipe, Trans. of the Korean Nuclear Society Autumn Meeting, Gyeongju, Korea, 2011.
- [15] O. Shoham, Flow pattern transition and characterization in gas-liquid two phase flow in inclined pipes, Ph.D. Thesis, University of Tel-Aviv, 1982.
- [16] T. Wu, Horizontal In-tube Condensation in the Presence of a Non-condensable Gas, Ph.D. Thesis, University of Purdue, 2005.
- [17] M. Kondo, and H. Nakamura, Primary-Side Two-Phase Flow and Heat Transfer Characteristics of a horizontal-tube PCCS Condenser, ICONE14-89652, 2006.